れず、移植部位において炎症細胞の浸潤が観られた。また、移植個体からブタiPS細胞に対する抗体が検出された。さらに、in vitroにおいてブタiPS細胞は、SLA合致ブタのNK細胞や補体などの自然免疫反応によって障害されることが明らかとなった。以上のことから、未分化なiPS細胞の残存による奇形腫形成の可能性は低いことが示された。一方で、ブタ同種移植実験系では、iPS細胞の生着および長期評価は出来なかった。

D. 考察

• ヒトiPS細胞のヒツジ胎仔への移植実験

肉眼的にグラフトを生着した大型動物を作製するために、未分化状態でヒトiPS細胞をヒツジ胎仔に移植することで、テラトーマの形成を試みた。すなわち、自殺遺伝子搭載あるいは非搭載ヒトiPS細胞を計6頭のヒツジ胎仔に移植した。その結果は、移植後に6例全て流産した。これに対し、ヒトiPS細胞株（線維芽細胞にレトロウイルスベクターを用いて作製したヒトiPS細胞株）を変更したところ、移植直後に流産せずに妊娠維持できた個体が3例得られた。いずれのiPS細胞においても、免疫不全マウスで成熟したテラトーマを形成することを確認している。それぞれの細胞株では、由来細胞やiPS細胞樹立用の遺伝子を導入する方法が異なる。移植後の流産の直接的な原因の解明を試みながら、妊娠が維持できるヒトiPS細胞株を用いて、ヒツジ胎仔への移植実験を続ける。

• SLA合致ブタを用いた移植実験

当初、ブタiPS細胞をSLA合致ブタに移植して奇形腫を作らせることを計画していたが、予想に反してSLAを合致させるだけではiPS細胞はブタに生着せず、奇形腫を形成しなかった(Mizukami Y, Abe T, et al. *PLOS ONE* 2014; 9:e98319)。このことから、ブタiPS細胞へ自殺遺伝子の搭載とSLA合致ブタへの移植実験は今後、本研究から除く。

E. 結論

平成26年度は、おおむね計画通り進捗している。SLA合致ミニブタへの同種移植実験系を除き、ヒトiPS細胞を用いたヒツジ胎仔への移植実験を引き続き進行中である。自殺遺伝子搭載iPS細胞に由来する分化細胞を生着した大型動物モデルの作製を進め、自殺遺伝子の有効性および安全性の評価をしていく。

G. 研究発表

1. 論文発表

1) **Abe T**, Hanazono Y, Nagao Y. A long-term follow-up study on the engraftment of human hematopoietic stem cells in sheep. *Exp Anim*. 2014;63(4):475-481.
2) Mizukami Y, **Abe T**, Shibata H, Makimura Y, Fujishiro SH, Yanase K, Hishikawa S, Kobayashi E, and Hanazono Y. MHC-matched induced pluripotent stem cells can attenuate cellular and humoral immune responses but are still susceptible to innate immunity. PLoS One. 2014;13;9(6):e98319.

2. 学会発表

1) 阿部朋行　サイエンティスト・クエスト～あなたと考えるあたらしい科学とくらし～（日本科学未来館）、2015 年 3 月 22 日
2) 阿部朋行、長尾慶和、原明日香、スブド・ビャンバー、柳瀬公秀、ボラジギン・サラントラガ、緒方和子、山口美緒、福森理加、花園豊　ヒツジ子宮内移植系におけるヒト造血細胞の生着促進・増幅技術の開発　第 17 回日本異種移植研究会　下野市　2015 年 3 月 14 日、抄録集 p.16
3) 阿部朋行　大動物を用いた再生医療研究～ヒト血液細胞をもつヒツジの作出　第 18 回予防衛生協会セミナー、つくば市、2015 年 2 月 14 日（抄録集 p.5）
4) 水上喜久、阿部朋行、柴田宏昭、牧村幸敏、藤城修平、柳瀬公秀、菱川修司、小林英司、花園豊　Transplantation-related Immunity of Porcine Induced Pluripotent Stem Cells in the MHC-matched Allogeneic Setting. 第 2 回日本先進医工学ブタ研究会（静岡県三島市）　2014 年 10 月 24-25 日
5) Tomoyuki Abe, Suvd Byambaa, Kimihide Yanase, Asuka Hara, Yoshikazu Nagao and Yutaka Hanazono. Hematopoietic Engraftment of Human iPS Cells in Sheep after in Utero Transplantation. 第 13 回 自治医科大学シンポジウム（下野市）　2014 年 9 月 5 日、講演要旨集 p.64
6) 水上喜久、阿部朋行、柴田宏昭、牧村幸敏、藤城修平、柳瀬公秀、菱川修司、小林英司、花園豊　Transplantation-related Immunity of Porcine Induced Pluripotent Stem Cells in the MHC-matched Allogeneic Setting. 第 13 回 自治医科大学シンポジウム（下野市）　2014 年 9 月 5 日、講演要旨集 p.47
7) 柳瀬公秀, 阿部朋行, Suvd Byambaa, 原明日香, 長尾慶和, 花園豊　ヒツジにおけるヒト造血の生着促進技術の開発　第 13 回 自治医科大学シンポジウム（下野市）　2014 年 9 月 5 日、講演要旨集 p.25
8) Yoshikazu Nagao, Tomoyuki Abe, Asuka

Hara, Kazuko Ogata, Mio Yamaguchi, Borjigin Sarentonglaga, Rika Fukumori and Yutaka Hanazono. Human hematopoietic re-constitution in ovine fetuses after in utero transplantation of human iPS cells. 17th International Congress on Animal Reproduction, Vancouver, July 29-August2, 2014. (Reproduction in Domestic Animals, Vol.47, s4, 589.)

9) Mizukami Y, **Abe T**, Shibata H, Makimura Y, Fujishiro SH, Yanase K, Hishikawa S, Kobayashi E, and Hanazono Y. Immune responses against induced pluripotent stem cells in porcine <HC-matched allogenic setting. Swine in Biomedical Research Conference. Raleigh, United States of America, July 6-8, 2014.

10) 阿部朋行、長尾慶和、柳瀬公秀、原明日香、ボラジギン・サラントラガ、緒方和子、山口美緒、花園豊　ヒツジ子宮内移植系におけるヒト造血細胞の生着・増幅技術の開発　第 61 回日本実験動物学会総会　札幌　2014 年 5 月 15-17 日　(抄録集 153)

H. 知的財産権の出願・登録状況

特になし。

Ⅲ．研究成果の刊行に関する一覧表

別紙４

研究成果の刊行に関する一覧表

雑誌

発表者氏名	論文タイトル名	発表誌名	巻号	ページ	出版年
Ayuso, E., Blouin, V., Lock, M., McGorray, S., Leon, X., Alvira, M. R., Auricchio, A., Bucher, S., Chtarto, A., Clark, K. R., Darmon, C., Doria, M., Fountain, W., Gao, G., Gao, K., Giacca, M., Kleinschmidt, J., Leuchs, B., Melas, C., Mizukami, H., Muller, M., Noordman, Y., Bockstael, O., Ozawa, K., Pythoud, C., Sumaroka, M., Surosky, R., Tenenbaum, L., van der Linden, I., Weins, B., Wright, J. F., Zhang, X., Zentilin, L., Bosch, F., Snyder, R. O., Moullier, P.	Manufacturing and characterization of a recombinant adeno-associated virus type 8 reference standard material.	Hum. Gene Ther.	25(11)	977-987	2014
Tsukahara, T., Iwase, N., Kawakami, K., Iwasaki, M., Yamamoto, C., Ohmine, K., Uchibori, R., Teruya, T., Ido, H., Saga, Y., Urabe, M., Mizukami, H., Kume, A., Nakamura, M., Brentjens, R., Ozawa, K.	The Tol2 transposon system mediates the genetic engineering of T-cells with CD19-specific chimeric antigen receptors for B-cell malignancies.	Gene Ther.	22(2)	209-215	2014
Uehara, T., Kanazawa, T., Mizukami, H., Uchibori, R., Tsukahara, T., Urabe, M., Kume, A., Misawa, K., Carey, T. E., Suzuki, M., Ichimura, K., Ozawa, K.	Novel anti-tumor mechanism of galanin receptor type 2 in head and neck squamous cell carcinoma cells.	Cancer Sci.	165(3)	72-80	2014
Wada, T., Koyama, D., Kikuchi, J., Honda, H. and Furukawa, Y.	Overexpression of the shortest isoform of histone demethylase LSD1 primes hematopoietic stem/progenitor cells for malignant transformation.	Blood		published online on April 22; doi:10.1182/blood-2014-11-610907	2015

Tago K, Funakoshi-Tago M, Itoh H, Furukawa Y, Kikuchi J, Kato T, Suzuki K, and Yanagisawa K	Arf tumor suppressor disrupts the oncogenic positive feedback loop including c-Myc and DDX5.	Oncogene	34	310-318	2015
Koyama D, Kikuchi J, Hiraoka N, Wada T, Kurosawa H, Chiba S, and Furukawa Y	Proteasome inhibitors exert cytotoxicity and increase chemosensitivity via transcriptional repression of Notch1 in T-cell acute	Leukemia	28	1216-1226	2014
Hiraoka N, Kikuchi J, Koyama D, Uesawa M, Akutsu M, Wada T, Abe M, Mori S, Nakamura Y, Kano Y, and Furukawa	Purine analog-like properties of bendamustine underlie rapid activation of DNA damage response and synergic effects with	PLoS One	9	e90675	2014
Kikuchi, J., Koyama, D., Mukai, H.Y. and Furukawa, Y.	Suitable drug combination with bortezomib for multiple myeloma under stroma-free conditions and in contact with fibronectin or bone marrow stroma.	Int. J. Hematol.	99	726-736	2014
Sripayap, P., Nagai, T., Hatano, K., Kikuchi, J., Furukawa, Y. and Ozawa, K.	Romidepsin overcomes cell adhesion-mediated drug resistance in multiple myeloma cells.	Acta Haematol.	132	1-4	2014
Abe T, Hanazono Y, Nagao Y.	A long-term follow-up study on the engraftment of human hematopoietic stem cells in sheep.	Exp Anim.	63(3)	475-481	2014
Mizukami Y, Abe T, Shibata H, Makimura Y, Fujishiro SH, Yanase K, Hishikawa S, Kobayashi E, and Hanazono Y.	MHC-matched induced pluripotent stem cells can attenuate cellular and humoral immune responses but are still susceptible to innate immunity.	PLoS One	9(6)	e98319	2014

Ⅳ. 研究成果の刊行物・別冊

（主なもの）

HUMAN GENE THERAPY 25:977–987 (November 2014)

DOI: 10.1089/hum.2014.057

Manufacturing and Characterization of a Recombinant Adeno-Associated Virus Type 8 Reference Standard Material

Eduard Ayuso,[1,*,†] Véronique Blouin,[2,3,*] Martin Lock,[4,*] Susan McGorray,[5] Xavier Leon,[1] Mauricio R. Alvira,[4] Alberto Auricchio,[6,7] Stephanie Bucher,[8] Abdelwahed Chtarto,[9,10] K. Reed Clark,[11,12] Christophe Darmon,[2,3,13] Monica Doria,[7] Will Fountain,[11,12] Guangping Gao,[14] Kai Gao,[14,15] Mauro Giacca,[16] Juergen Kleinschmidt,[17] Barbara Leuchs,[17] Catherine Melas,[9,10] Hiroaki Mizukami,[18] Marcus Müller,[17] Yvet Noordman,[19] Olivier Bockstael,[9,10] Keiya Ozawa,[18] Catherine Pythoud,[20] Marina Sumaroka,[21] Richard Surosky,[22] Liliane Tenenbaum,[20] Inge van der Linden,[19] Brigitte Weins,[23] J. Fraser Wright,[21,24] Xinhua Zhang,[21] Lorena Zentilin,[16] Fatima Bosch,[1] Richard O. Snyder,[25–27] and Philippe Moullier[2,3,27]

Abstract

Gene therapy approaches using recombinant adeno-associated virus serotype 2 (rAAV2) and serotype 8 (rAAV8) have achieved significant clinical benefits. The generation of rAAV Reference Standard Materials (RSM) is key to providing points of reference for particle titer, vector genome titer, and infectious titer for gene transfer vectors. Following the example of the rAAV2RSM, here we have generated and characterized a novel RSM based on rAAV serotype 8. The rAAV8RSM was produced using transient transfection, and the purification was based on density gradient ultracentrifugation. The rAAV8RSM was distributed for characterization along with standard assay protocols to 16 laboratories worldwide. Mean titers and 95% confidence intervals

[1]Center of Animal Biotechnology and Gene Therapy and Department of Biochemistry and Molecular Biology, School of Veterinary Medicine, Universitat Autònoma de Barcelona, 08193-Bellaterra, Spain.
[2]INSERM UMR1089, CHU de Nantes 44000, France.
[3]Atlantic Gene Therapies, Nantes 44000, France.
[4]Gene Therapy Program, Department of Pathology and Laboratory Medicine, University of Pennsylvania, Philadelphia, PA 19104.
[5]Department of Biostatistics, Colleges of Medicine and Public Health and Health Professions, University of Florida, Gainesville, FL 32610-0177.
[6]Medical Genetics, Department of Translational Medicine, "Federico II" University, Napoli 80131, Italy.
[7]Telethon Institute of Genetics and Medicine, TIGEM, 80131 Napoli, Italy.
[8]GENETHON, 1bis rue de l'Internationale, 91000 Evry, France.
[9]Laboratory of Experimental Neurosurgery, Free University of Brussels, Brussels 1070, Belgium.
[10]Multidisciplinary Research Institute, Free University of Brussels, Brussels 1070, Belgium.
[11]Center for Gene Therapy, The Research Institute at Nationwide Children's Hospital, Columbus, OH 43205.
[12]Department of Pediatrics, The Ohio State University, Columbus, OH 43210.
[13]EFS-Atlantic BioGMP, Nantes 44800, France.
[14]Gene Therapy Center, University of Massachusetts Medical School, Worcester, MA 01605.
[15]Division of Biopharmaceuticals, National Institute for Food and Drug Control, Beijing 100050, China.
[16]Molecular Medicine Laboratory, International Centre for Genetic Engineering and Biotechnology (ICGEB), Padriciano, 34149 Trieste, Italy.
[17]Research Program Infection and Cancer, German Cancer Research Center, Heidelberg 69120, Germany.
[18]Division of Genetic Therapeutics, Center for Molecular Medicine, Jichi Medical University, Tochigi 329-0498, Japan.
[19]uniQure, Amsterdam 1100, The Netherlands.
[20]Laboratory of Cellular and Molecular Neurotherapies and Neurosurgery Service, Department of Clinical Neurosciences, Lausanne University Hospital, Lausanne 1015, Switzerland.
[21]Center for Cellular and Molecular Therapeutics, Children's Hospital of Philadelphia, Philadelphia, PA 19104.
[22]Sangamo Biosciences, Inc., Richmond, CA 94804.
[23]Progen Biotechnik GmbH, 69123 Heidelberg, Germany.
[24]Department of Pathology and Laboratory Medicine, University of Pennsylvania School of Medicine, Philadelphia, PA 19104.
[25]Center of Excellence for Regenerative Health Biotechnology, University of Florida, Gainesville, FL 32611-0585.
[26]Division of Cellular and Molecular Therapy, Department of Pediatrics, University of Florida, Gainesville, FL 32610.
[27]Department of Molecular Genetics and Microbiology, University of Florida College of Medicine, Gainesville, FL 32610.
*These three authors contributed equally to this work.
†Present address: INSERM UMR1089, CHU de Nantes 44000, France and Atlantic Gene Therapies, Nantes 44000, France.

were determined for capsid particles (mean, 5.50×10^{11} pt/ml; CI, 4.26×10^{11} to 6.75×10^{11} pt/ml), vector genomes (mean, 5.75×10^{11} vg/ml; CI, 3.05×10^{11} to 1.09×10^{12} vg/ml), and infectious units (mean, 1.26×10^{9} IU/ml; CI, 6.46×10^{8} to 2.51×10^{9} IU/ml). Notably, there was a significant degree of variation between institutions for each assay despite the relatively tight correlation of assay results within an institution. This outcome emphasizes the need to use RSMs to calibrate the titers of rAAV vectors in preclinical and clinical studies at a time when the field is maturing rapidly. The rAAV8RSM has been deposited at the American Type Culture Collection (VR-1816) and is available to the scientific community.

Introduction

REMARKABLE CLINICAL SUCCESSES have been achieved in humans using recombinant adeno-associated viral (rAAV) vectors for hemophilia B, Leber congenital amaurosis,, and lipoprotein lipase deficiency (LPLD), among other diseases (Manno *et al.*, 2006; Bainbridge *et al.*, 2008; Maguire *et al.*, 2008; Nathwani *et al.*, 2011; Gaudet *et al.*, 2013). AAV serotype 2 is so far the best characterized and most used serotype for gene transfer studies, but other AAV serotypes with more efficient gene delivery profiles for specific tissues are currently in human trials and their use will likely increase. One example is the clinical trial for hemophilia B using rAAV serotype 8 that has shown long-term expression of the transgene by the liver with significant clinical benefit (Nathwani *et al.*, 2011). The market authorization by the European Medicine Agency in 2012 of Glybera, an rAAV1 vector for the treatment of LPLD patients, was a milestone in the field of gene therapy and prompted many pharmaceutical companies to move into this field (Bryant *et al.*, 2013).

As the first reference standard initiative in the viral vector gene therapy field, an Adenovirus Reference Material Working Group was established and generated a human adenovirus 5 Reference Standard Material (RSM; ATCC VR-1516) in 2002 (Hutchins, 2002). A similar need was recognized associated with the use of rAAV relating to the inability to calibrate vector doses administered by different investigators to animals and humans. The need for RSMs for AAV vectors was recognized by the research community, and an AAVRSM Working Group was established and committed to the development of an rAAV2 Reference Standard Material (rAAV2RSM) (Snyder *et al.*, 2002). The AAVRSM Working Group is a volunteer organization and comprises members from both industry and universities, under the guidance of the FDA and NIH (Moullier *et al.*, 2008, 2012). The AAVRSM Working Group decided in 2002 that the first AAV RSM had to be based on the prototypical AAV serotype 2. Thus, the rAAV2RSM was produced by cotransfection of HEK293 cells with an AAV2 genome/hGFP transgene plasmid and a second plasmid encoding the AAV2 replication and capsid proteins, and was purified by sequential rounds of column chromatography (Potter *et al.*, 2008).

The rAAV2RSM was characterized by 16 laboratories worldwide, the data were published, and this material is available for the scientific community through the American Tissue Culture Collection (ATCC; VR-1616) (Lock *et al.*, 2010). Following this example, another effort was initiated by the AAVRSM Working Group in 2008 to generate a novel RSM based on serotype 8 (Gao *et al.*, 2002). The rAAV8RSM Working Group included members who participated in the AAV2RSM effort from industry and academia, from Europe, United States, and Japan (Moullier *et al.*, 2008). The rAAV8RSM was initiated in the framework of the European Clinigene Network of Excellence. The rAAV8RSM was manufactured in Europe by two laboratories (Atlantic Gene Therapies at Nantes, France, and the Center of Animal Biotechnology and Gene Therapy at the Universitat Autonoma de Barcelona, Spain), and the characterization of the material involved 16 laboratories worldwide (coordinated by the University of Florida and the University of Pennsylvania). The rAAV8RSM is a pseudotyped AAV2 genome vector with capsid serotype 8 (Gao *et al.*, 2002) expressing the GFP protein. To harmonize the two reference standards, the rAAV8RSM contains the same vector genome that was used for the rAAV2RSM. The vector was also produced by cotransfection of HEK293 cells, but the purification step differed from the rAAV2RSM, as it was purified by density ultracentrifugation using an optimized cesium chloride (CsCl) gradient-based protocol (Ayuso *et al.*, 2012) and formulated in dPBS at a target concentration of $>10^{11}$ vg/ml in cryovials frozen at EFS-Atlantic Bio-GMP.

The protocols for the characterization were based on the previously developed consensual protocols for the rAAV2RSM but adapted to serotype 8 (ATCC Virus Reference Materials). The rAAV8RSM characterization assays performed by the 16 laboratories included (1) capsid titer by enzyme-linked immunosorbent assay (ELISA); (2) vector genome titer by quantitative polymerase chain reaction (qPCR); (3) infectious titer by medium tissue culture infective dose ($TCID_{50}$) with qPCR readout; and (4) purity by sodium dodecyl sulfate–polyacrylamide gel electrophoresis (SDS-PAGE). The AAV8RSM was also tested for sterility, endotoxin, and mycoplasma. Altogether, this international effort led to the generation of more than 4040 vials of an rAAV8RSM that is stored at ATCC (No. VR-1816) and is available to the community.

Finally, to cross-validate the use of the AAVRSMs, we conducted a side-by-side comparison of rAAV2RSM versus rAAV8RSM in terms of vector genome titration and capsid content using non-serotype-dependent techniques. The data generated by four laboratories within the AAV8RSM Working Group were in agreement with the mean values reported by the community for the rAAV2RSM (Lock *et al.*, 2010) and the rAAV8RSM (data from this article).

Materials and Methods

Reference standard material manufacturing

Production and purification of the rAAV8RSM were carried out at Atlantic Gene Therapies–UMR 1089 in Nantes (France) and the Center of Animal Biotechnology and Gene Therapy (CBATEG) at the Universitat Autonoma de Barcelona (Spain).

Production was initiated by co-transfection of a certified master cell bank of HEK293 cells (ABG-EFS) in five-chamber Corning Cellstacks (at Nantes) or Corning Roller Bottles with plasmid pTR-UF-11 (ATCC # MBA-331), containing the vector genome and hGFP expression cassette (Burger *et al.*, 2004) and the pDP8 helper plasmid harboring the *rep* gene from AAV2, the *cap* gene from AAV8, the adenovirus helper genes *E2A*, *E4*, and *VA-RNA*, and the ampicillin resistance gene (No. PF478; Plasmidfactory) using a calcium phosphate precipitation method. Same lots of FBS (Hyclone-Thermo scientific), trypsin (PAA Laboratories GmbH), DMEM (PAA), Pen/Strep (PAA), PBS (PAA), and dPBS (PAA) were split between the two manufacturing sites.

For the transfection, the complete medium (DMEM, 10% FBS, 1% Pen/Strep) was removed and replaced by a transfection medium (DMEM, 2% FBS, 1% Pen/Strep) including the transfection mixture. After 6–15 hr at 37°C and 5% CO_2, the transfection medium was then removed and replaced by a fresh exchange medium (DMEM, 1% Pen/Strep) before 3 days of incubation at 37°C and 5% CO_2. The cells were harvested and centrifuged at 1500 *g* for 10 min at 4°C. The cell pellet was discarded and the supernatant was precipitated with PEG at a final concentration of 8% for a period of 15 hr to 3 days at 5 ± 3°C. Samples of these cell pellets from Nantes and Barcelona were tested for mycoplasma and found to be negative by PCR using the Mycotrace kit (PAA, ref: Q052-20). The PEG-precipitated supernatant was then centrifuged at 5000 *g* for 45 min at 4°C. The supernatant was discarded and the PEG-pellet was resuspended in tris buffer saline before benzonase digestion at 37°C for 30 min.

Following benzonase digestion, the viral suspension was centrifuged at 10,000 *g* for 10 min at 4°C and the vector-containing supernatant was loaded on a step density CsCl gradient (1.5 g/cm^3 at the bottom and 1.3 g/cm^3 on top) in UltraClear tube for SW28 rotor (Beckman Coulter). The gradient was centrifuged at 28,000 rpm for 24 hr at 15°C. The full particles band was collected with a 10 ml syringe and transferred to a new UltraClear tube for SW41 rotor filled with 1.375 g/cm^3 density CsCl. The second gradient was centrifuged at 38,000 rpm for 48 hr at 15°C. The enriched full particle band was then collected with a 10 ml syringe (the volume recovered for each run is indicated in Supplementary Tables S1 and S2; Supplementary Data are available online at www.liebertpub.com/hum). The viral suspension was then subjected to four successive rounds of dialysis under slight stirring in a Slide-a-Lyzer cassette (Pierce) against dPBS (containing Ca and Mg). No other additives were included in the formulation buffer (dPBS).

Each purified vector sublot was finally collected, sampled for vg titer and purity assay, and stored at less than −70°C in polypropylene low-binding cryovials.

The specifications of the dPBS (PAA Laboratories) used as a formulation buffer were as follows:

pH 7.0–7.5
Osmolality 240–320 mOsmol/kg
Endotoxin < 1 EU/ml
Composition: KCL 0.2 g/l; KH_2PO_4 0.2 g/l; NaCl 8.00 g/l; Na_2HPO_4 anhyd. 1.15 g/l; $CaCl_2$–$2H_2O$ 0.132 g/l; $MgCl_2$–$2H_2O$ 0.1 g/l.

rAAV8RSM fill finish and final quality control

Fill finish and final quality control (QC) were carried out at EFS-ABG, a European pharmaceutical site dedicated to ATMPs manufacturing. All of the sublots produced at Nantes and Barcelona (except two lots, as described in the Results section) were combined and diluted to 200 ml in dPBS (see specifications and composition above). This purified bulk was subsequently tested for endotoxin (EP 2.6.14), mycoplasma (EP 2.6.7), and bioburden (EP 2.6.12) by Vitrology Ltd., and the vector genome titer was determined by qPCR at Atlantic Gene Therapies, before final formulation, sterile filtration, and filling in an ISO5 cleanroom at EFS-ABG with environmental monitoring. The purified bulk was diluted with 325 ml of dPBS and was then sterile-filtered using a 0.2 μm PES filter (Sartorius). The filtered formulated bulk was then vialed in 14 sterile 50 ml conical tubes (Corning; polypropylene 50 ml tubes, USP class VI) stored at less than −70°C. The sterile bulk was then filled into 4088 cryovials (Corning; 1.2 ml polypropylene cryogenic vial, USP class VI) with a volume of 0.125 ml/vial using an electronic adjustable repeating pipette AutoRep (Rainin). Before storage at less than −70°C, the vials were labeled according to ATCC requirements as follows: ATCC, VR-1816, rAAV8-RSS—Reference Material, ABG[date] −0.125 ml, Store at less than −70°C—For research use only. Lot #03112010SP2pcg.

Due to the number of vials (>4000 vials), seven fill days were required. Each fill date is indicated on the label. At each filling session, the first and the last cryovials filled were transferred to QC for further sterility assay. Thus, a total of 28 cryovials were submitted to sterility assay at Vitrology Ltd. The final product was submitted to preliminary tests for vector genome titer (qPCR SV40 and dot blot hybridization using a GFP probe), transducing titer, and purity/identity (silver-stained SDS-PAGE gel). A summary of QC performed on the purified bulk and on the final product is shown in Table 1. The SDS-PAGE silver stain purity assay is shown in Supplementary Fig. S1 and suggests that the AAV8RSM purity is similar to the control AAV2RSM, one which was determined at 94% using Sypro Ruby staining following SDS-PAGE (Lock *et al.*, 2010).

rAAV8 RSM handling. For rAAV8RSM characterization, each testing laboratory received two vials from ATCC on dry ice. Upon receipt, both vials were stored frozen at −70°C to −90°C. One vial was thawed at room temperature while mixing gently and then kept on wet ice. Within 1 hr of thawing, the infectious titer was conducted. The remainder of the thawed vial was stored at 4°C and mixed gently upon use. Within 5 days of vial thaw, the particle titer, vector genome titer, and purity/identity assays were performed. These steps were repeated for the second vial starting on a different calendar day.

rAAV8RSM characterization assays

Brief descriptions of each characterization assay follow. For those wishing to reproduce these assays, detailed protocols can be requested directly from M. Lock or R. Snyder.

Particle titer. The particle concentration was determined by each laboratory, using four separate dilution series from a single vial in the Progen AAV8 Titration ELISA (Progen

TABLE 1. QUALITY CONTROL OF INTERMEDIATE AND FINAL PRODUCT

Test item	*Tests*	*Method*	*Laboratory*	*Results*
Purified bulk	Vector genome (vg/ml)	qPCR	UMR1089	5.7×10^{12} vg/ml
	Bioburden	EP 2.6.12	SGS-Vitrology	0 cfu/ml
	Endotoxin	EP 2.6.14	SGS-Vitrology	<0.03 EU/ml
	Mycoplasma	EP 2.6.7	SGS-Vitrology	Negative
Final product	Vector genome (vg/ml)	qPCR	UMR1089	6.4×10^{11} vg/ml
	Vector genome (vg/ml)	Dot blot	UMR1089	6.3×10^{11} vg/ml
	Transducing units (TU/ml)	Transduction of cells; GFP read out	UMR1089	1.5×10^{8} TU/ml
	Sterility	EP 2.6.1	SGS-Vitrology	Sterile

qPCR, quantitative polymerase chain reaction.

Biotechnik GMBH; Article number PRAAV8), against a standard curve prepared from a previously titered rAAV8 preparation (WL217S). The particle content of WL217S was determined by first spiking the preparation with the adenoviral reference material (ARM ATCC VR-1516, with a known particle concentration) and then obtaining images of the particles by electron microscopy. Because of the size difference between AAV and adenovirus, the particles of each can be distinguished and counted on electron micrographs. Several fields were counted, and the average ratio of AAV particles to the internal ARM standard was used to compute the particle titer for WL217S.

Vector genome titer. The vector genome concentration was determined in duplicate, testing one replicate from each of two vials, by qPCR of serial dilutions of rAAV8RSM against a standard curve of plasmid pTR-UF-11 (ATCC MBA-331) (Burger *et al.*, 2004). Some labs performed more than two tests for vector genome titrations (Table 3).

Infectious titer. Serial 10-fold dilutions of rAAV8RSM were made on HeLa RC32 cells (ATCC CRL-2972) (Tessier *et al.*, 2001) and co-infected with adenovirus type 5 (ATCC VR-1516). Seventy-two hours after infection, total cell DNA was extracted and analyzed for AAV vector genome copies by qPCR. Input vector genomes were subtracted and $TCID_{50}$ titers calculated according to the method of Spearman–Karber.

Purity and identity. The purity and identity of the rAAV8RSM were evaluated by SDS-PAGE, using Sypro Ruby (Invitrogen) or silver staining (SilverXpress; Invitrogen). The AAV8 VP1, VP2, and VP3 capsid protein bands were evaluated for their stoichiometry and size. Purity relative to nonvector impurities visible on stained gels was determined.

Results

rAAV8RSM manufacturing and predistribution QC

The manufacturing of the rAAV8RSM was carried out by two laboratories that harmonized their production protocols: Atlantic Gene Therapies–UMR 1089 in Nantes (France) and the Center of Animal Biotechnology and Gene Therapy (CBATEG) at the Universitat Autonoma de Barcelona (Spain).

The rAAV8RSM is an rAAV vector serotype 8 (Gao *et al.*, 2002) produced using a HEK293 transfection-based protocol. HEK293 cells were amplified from a cGMP master cell bank and transfected by the vector plasmid pTR-UF11 (Burger *et al.*, 2004), the same plasmid used to generate the rAAV2RSM (Potter *et al.*, 2008; Lock *et al.*, 2010), and the pDP8 helper plasmid (see Materials and Methods section: Reference standard material manufacturing). Twelve sublots of rAAV8RSM were produced and purified in France and 15 sublots in Spain. The protocol followed was previously described (Ayuso *et al.*, 2010). Since it was known that up to 80% of functional rAAVs from serotype 8 are released into cell culture supernatant (Vandenberghe *et al.*, 2010), the cell pellet was discarded and the supernatant was processed by PEG precipitation and subsequently purified by double-cesium-chloride (CsCl) gradient ultracentrifugations followed by a dialysis step against phosphate buffered saline containing calcium and magnesium (dPBS) (Fig. 1).

In-process QC testing was performed on each sublot for purity, identity, and vector genome titer to meet predetermined minimum specifications: (1) >85% purity and the correct AAV capsid protein banding pattern and (2) vector genome titer $>10^{12}$ vg/ml. Silver staining of SDS-PAGE gel of each sublot is shown in Supplementary Fig. S2. The sublot BCN7 was discarded because of the presence of significant impurities (Supplementary Fig. S2B). Identity of the VP proteins was verified on a few sublots by Western blot analysis using anti-capB1 or anti-AAV2 polyclonal antibodies (Supplementary Fig. S2C). The Western blot analysis using a polyclonal anti-AAV2 antibody suggests that the extra-band migrating below VP3 revealed by silver stain (Supplementary Fig. S2A) is a cleavage product of the capsid proteins (Van Vliet *et al.*, 2006). The vector genome titer was determined in each sublot by dot-blot and/or qPCR using the rAAV2RSM as a control (Supplementary Tables S1 and S2).

The sublot BCN4 was discarded because of the vector genome titer being below the target concentration. Accordingly, a total of 25 selected sublots were then combined and diluted with dPBS to generate the purified bulk. The purified bulk was then tested for vector genome titer, bioburden, mycoplasma, and endotoxin before fill and finish (Table 1). A total of 4088 vials containing 0.125 ml were subsequently filled into 1.2 ml polypropylene low-binding cryovials. Vector genome and infectious titers (transducing units) as well as microbiological tests were performed on the final product before shipment to the American Type Culture Collection (catalog no. VR-1816) (Table 1). In summary, we

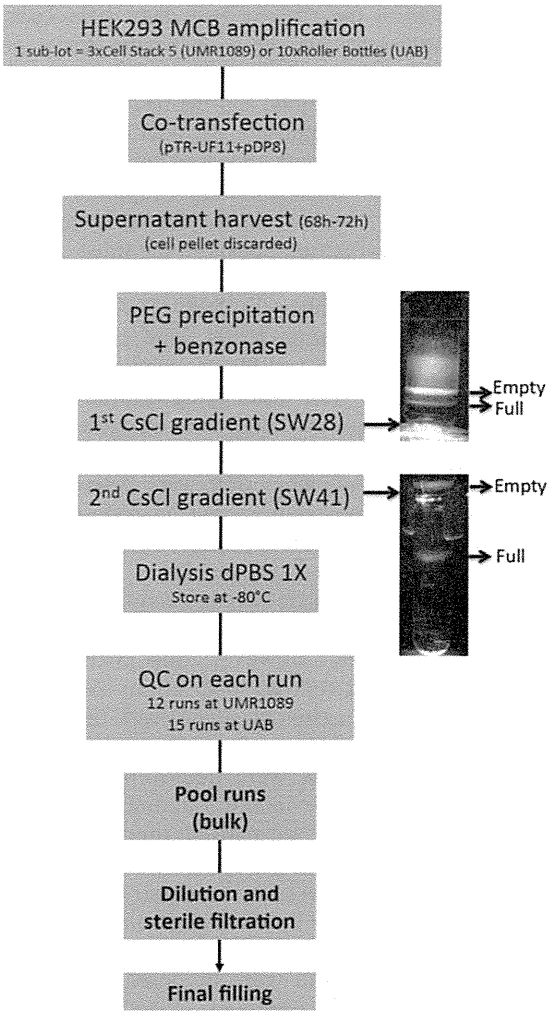

FIG. 1. Flow chart showing the steps of rAAV8RSM manufacturing. Note the pictures on the right showing the empty and full vector particle bands at the first and second CsCl gradient step. MCB, master cell bank; PEG, polyethylene glycol; QC, quality control; rAAV8, recombinant adeno-associated virus serotype 8; RSM, Reference Standard Materials.

generated about 500 ml of rAAV8RSM with an estimated titer of 6×10^{11} vg/ml, resulting in a total vector amount of $>3\times10^{14}$ vg.

Characterization of the rAAV8RSM

For the characterization of the rAAV8RSM, we took advantage of the experience previously gained when the community characterized the rAAV2RSM, and therefore we used similar protocols and reagents adapted to the AAV8 serotype. The assays chosen for the rAAV8RSM characterization included (1) confirmation of the serotype and capsid particle titer by an AAV8-specific ELISA (Progen) (Sonntag *et al.*, 2011); (2) vector genome titer by qPCR; (3) infectious titer by tissue culture infective dose ($TCID_{50}$) with qPCR readout; (4) evaluation of the purity, capsid subunit stoichiometry, and chemical integrity of the capsid by SDS-PAGE.

Key reagents used for the characterization of the rAAV 8RSM were already used for the rAAV2RSM characterization and are available from ATCC. For both genome and infectious titers assays, a qPCR primer–probe set directed to the SV40 polyA sequence and a dilution series specific to the RSM were selected. For the purity and identity assay, commercially available assay reagents with the highest sensitivity were suggested. Using these reagents, the protocols were adapted for rAAV8 vectors and were beta-tested at the University of Pennsylvania Gene Therapy Program against both in-house standards and the rAAV8RSM itself. The finalized protocols were posted on the ATCC website.

The rAAV8RSM (ATCC VR-1816) was distributed along with the required reagents and handling instructions to 16 laboratories worldwide (Table 2), which volunteered to conduct one or more of the characterization assays. The characterization phase of the rAAV8RSM proceeded from 2011 to 2013. Upon receipt, the RSM was evaluated by the 16 testing laboratories according to the posted protocols, and the data were recorded on the assay spread sheets provided, which contained the necessary calculations for titer determination.

The raw data that emerged from the testing laboratories for the three quantitative titer assays (Table 3) were statistically analyzed to determine true mean titer values and 95% confidence intervals. The distribution was first visualized as histograms (Supplementary Fig. S3), and it was noted that the data did not appear to be normally distributed. Since valid estimation of the mean and confidence interval relies on an underlying normal distribution, it was clear that some form of transformation was warranted. Common statistical transformation methods employed are square root, natural log, and log base 10. Therefore, means and intervals were calculated on the transformed data, and the results were then back-transformed to the original measurement scale; the data for each assay were processed in this way using all three transformations. Analysis of the mean and median (for normally distributed data, these two values are the same) and skewness and kurtosis estimates confirmed that the transformations were performing as expected and were

TABLE 2. rAAV8 REFERENCE STANDARD MATERIAL TESTING LABORATORIES

Telethon Institute of Genetics and Medicine, TIGEM, Italy
Universitat Autonoma de Barcelona, Spain
Research Institute at Nationwide Children's Hospital, USA
University of Florida, USA
Atlantic Gene Therapies, France
Genethon, France
International Center for Genetic Engineering and Biotechnology (ICGEB), Italy
German Cancer Research Center (DKFZ), Germany
University of Pennsylvania, USA
Jichi Medical University, Japan
Sangamo BioSciences, USA
University of Massachusetts Medical School, USA
Universite Libre de Bruxelles, Belgium
uniQure, The Netherlands
Children's Hospital of Philadelphia, USA
Lausanne University Hospital, Switzerland

rAAV8, recombinant adeno-associated virus serotype 8.

TABLE 3. rAAV8 REFERENCE STANDARD MATERIAL RAW CHARACTERIZATION DATA

Laboratory	*Replicate*	*Particle titer (ELISA) (pt/ml)*	*Genome titer (qPCR) (vg/ml)*	*Infectious titer (TCID50) (IU/ml)*
A	1	2.68×10^{11}	3.60×10^{11}	**1.65×10^{11}**
	2	2.08×10^{11}	4.58×10^{11}	**1.36×10^{11}**
	3		2.46×10^{11}	**1.36×10^{11}**
B	1	**5.39×10^{13}**	3.47×10^{12}	
	2	**9.11×10^{13}**	4.73×10^{12}	
C	1	8.25×10^{11}	5.53×10^{11}	9.28×10^{9}
	2	5.68×10^{11}	3.39×10^{11}	9.28×10^{9}
	3		3.42×10^{11}	1.12×10^{10}
D	1	6.03×10^{11}	5.19×10^{11}	2.00×10^{9}
	2	8.90×10^{11}	8.50×10^{11}	1.65×10^{9}
E	1	4.88×10^{11}	6.32×10^{11}	1.65×10^{9}
	2	5.53×10^{11}	3.00×10^{11}	1.82×10^{9}
F	1	4.57×10^{11}	7.71×10^{10}	5.22×10^{9}
	2	3.81×10^{11}	7.58×10^{10}	4.74×10^{9}
	3		8.14×10^{10}	
G	1	8.08×10^{11}	1.18×10^{12}	3.23×10^{9}
	2	4.73×10^{11}	1.02×10^{12}	5.22×10^{9}
	3		9.60×10^{11}	4.74×10^{9}
H	1		3.10×10^{12}	6.32×10^{8}
	2		2.64×10^{12}	2.42×10^{8}
I	1	6.26×10^{11}	9.56×10^{11}	6.32×10^{8}
	2	7.40×10^{11}	8.25×10^{11}	4.31×10^{8}
	3		7.19×10^{11}	
	4		4.86×10^{11}	
	5		5.39×10^{11}	
J	1		2.24×10^{12}	
	2		2.40×10^{12}	
K	1	4.77×10^{11}	7.02×10^{10}	
	2	5.52×10^{11}	4.65×10^{10}	
L	1	4.35×10^{11}	7.45×10^{11}	5.22×10^{8}
	2	4.13×10^{11}	3.29×10^{11}	
	3		8.79×10^{11}	
	4		4.20×10^{11}	
M	1	3.17×10^{11}	7.06×10^{11}	1.65×10^{9}
	2	2.45×10^{11}	8.58×10^{11}	9.28×10^{8}
	3		5.28×10^{11}	
	4		2.26×10^{11}	
N	1	1.09×10^{12}	1.55×10^{11}	1.12×10^{9}
	2	8.73×10^{11}	1.57×10^{11}	4.31×10^{8}
O	1	6.22×10^{11}	2.61×10^{12}	5.75×10^{8}
	2	6.22×10^{11}	3.53×10^{12}	3.56×10^{8}
P	1	3.19×10^{11}	2.59×10^{11}	6.32×10^{8}
	2	4.51×10^{11}	3.73×10^{11}	2.67×10^{8}
	3		3.48×10^{11}	9.28×10^{8}
Mean		5.50×10^{11}	9.62×10^{11}	2.67×10^{9}
SD		2.20×10^{11}	1.10×10^{12}	3.32×10^{9}

Numbers in bold were considered outlyers.

similar to those obtained for the AAV2RSM (Supplementary Table S3).

Supplementary Fig. S4 shows the results of the most successful transformations for each assay as quantile–quantile plots. In this analysis, the quantiles (i.e., 5%, 10%, etc.) obtained from the transformed data were compared with the quantiles that would be expected for a normal distribution. A line that extends through the 25th and 75th quantile is shown on the plots, and the nearer the points are to this line, the more normal are the data distribution. The capsid particle titer assay data appeared normally distributed without the need for transformation (Supplementary Fig. S4a). For the vector genome titer and for the infectious titer, a log base 10 transformation appeared the most appropriate (Supplementary Fig. S4b and c). The transformed data are summarized in Supplementary Table S4. For each assay, two and three standard deviation limits were calculated corresponding to nominal 95% and 99.7% confidence bounds on individual values. Any test result lying outside of the three standard deviations was considered to be an outlier. Using this criterion, only one test result from the particle titer assay and one test result from infectious titer were determined to be outliers and were removed from the analysis (Table 3, in bold); the values reported in Supplementary Table S4 exclude these data points.

An assumption we made when calculating the mean values and confidence intervals is that each test result is independent of another; however, this assumption does not take into account that all institutions submitted duplicate (and in some cases triplicate) test results for the assays. To assess the degree of correlation between samples, Pearson coefficients were determined for the first two duplicate samples per institution, and the coefficients obtained were 0.71 for vector particle titer, 0.96 for vector genome titer, and 0.97 for infectious units titer. These results indicated that there was a significant correlation within institutions and that the assumption that each result is independent was violated. To account for this correlation, the transformed data were modeled, using a linear random effect modeling approach (Littell *et al.*, 2006). This allows for a unique component associated with each institution to be included in the model, under the assumption that these institutional random effects have a mean of zero. When the correlation within an institution is accounted for, the precision of the mean estimate as illustrated by the width of the 95% confidence interval is decreased (Table 4). Taking the transformed, modeled data as the true estimate of the mean, we reached the following determinations for the rAAV8RSM: the mean particle titer is 5.5×10^{11} pt/ml, with 95% confidence that the true value lies in the range 4.26×10^{11} to 6.75×10^{11} pt/ml; the mean vector genome titer is 5.75×10^{11} vg/ml, with 95% confidence that the true value lies in the range 3.05×10^{11} to 1.09×10^{12} vg/ml; and the mean infectious titer is 1.26×10^{9} $TCID_{50}$ IU/ml, with 95% confidence that the true value lies in the range 6.46×10^{8} to 2.51×10^{9} $TCID_{50}$ IU/ml (Table 4).

Interestingly, the vector genome titer was very similar to the vector particle titer, indicating that the AAV8RSM is virtually devoid of empty particles. This finding is consistent with the CsCl gradient purification protocol used in the production of the rAAV8RSM that efficiently separates empty versus full particles (Ayuso *et al.*, 2010).

The DNA content of the AAV8RSM was extracted and native agarose gel electrophoresis was used to confirm the homogeneity and the size of the vector genome (expected genome size of 4.3 kb) (Supplementary Fig. S5).

TABLE 4. FINAL rAAV8 REFERENCE STANDARD MATERIAL TITER ESTIMATES AFTER TRANSFORMATION AND MODELING

Titer units	*Transformation*	*Mean*	*Lower 95% confidence limit for the mean*	*Upper 95% confidence limit for the mean*	*±2 SD*
Particles (pt)/ml	None	5.5×10^{11}	4.26×10^{11}	6.75×10^{11}	1.06×10^{11} to 9.94×10^{11}
Vector genomes (vg)/ml	Log_{10}	5.75×10^{11}	3.05×10^{11}	1.09×10^{12}	4.57×10^{10} to 7.24×10^{12}
Infectious units (IU)/ml	Log_{10}	1.26×10^{9}	6.46×10^{8}	2.51×10^{9}	1.32×10^{8} to 1.20×10^{10}

The purity of the rAAV8RSM was assessed by SDS-PAGE analysis. The RSM was examined under both denaturating and nondenaturating conditions using Sypro Ruby and silver stains (Fig. 2). Under denaturating conditions, all proteins including the denatured AAV8 capsids are expected to enter the gel, and impurities would be detected as protein bands other than the capsid proteins VP1, VP2, and VP3. Under nondenaturating conditions, the capsid would remain intact and would not be expected to enter the resolving gel, whereas impurities would enter the gel; proteins, which previously comigrated with the capsid proteins on denaturating gels, would thus be detected. Silver nitrate staining was included since it is capable of detecting DNA, lipid, and carbohydrate impurities as well as nanogram levels of protein (Weiss *et al.*, 2009). Sypro Ruby is a protein-specific fluorescent dye that has sensitivity close to that of silver stain (Rabilloud *et al.*, 2001; Weiss *et al.*, 2009). In each case, the rAAV8RSM was analyzed alongside an internal laboratory-standard AAV vector. The consensus data from the 14 testing laboratories that carried out the purity test estimated that the rAAV8RSM was greater than 99% pure and confirmed that VP1, VP2, and VP3 co-migrated with the

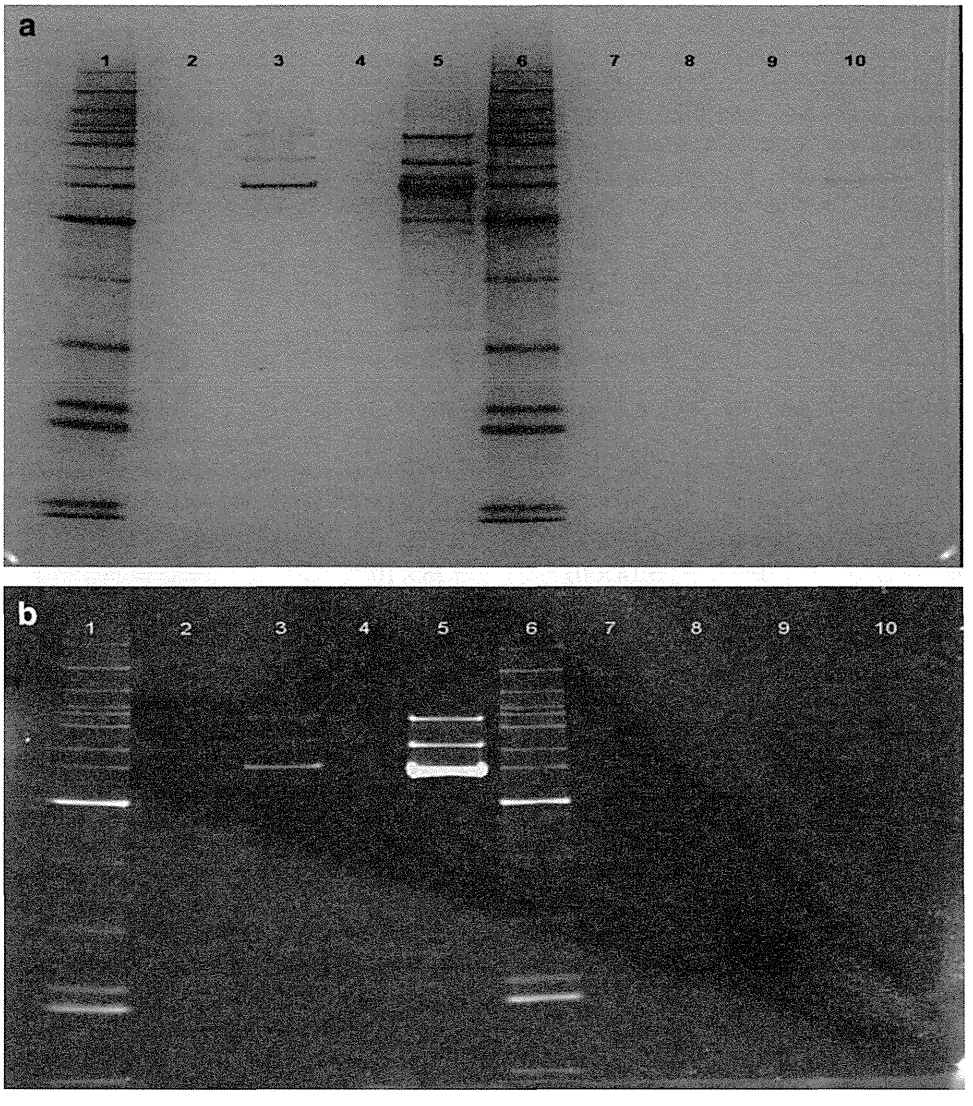

FIG. 2. The rAAV8RSM was run on SDS-PAGE gels under both denaturating and native conditions and then stained with **(a)** silver stain and **(b)** Sypro Ruby. In-house rAAV standard was run as a positive control and buffer as a negative control. The lanes for each gel are (1) benchmark ladder (unstained or prestained)—reduced; (2) negative control—reduced; (3) AAV8 reference material—reduced; (4) empty; (5) positive control—reduced; (6) benchmark ladder (unstained or prestained)—native; (7) negative control—native; (8) AAV reference material—native; (9) empty; and (10) positive control—native. SDS-PAGE, sodium dodecyl sulfate–polyacrylamide gel electrophoresis.

AAV capsid proteins of the internal vector standards (Fig. 2 and data not shown).

Comparison of rAAV2RSM versus rAAV8RSM

Having an increasing repertoire of AAV serotypes entering the clinical arena is encouraging for the field of AAV-mediated gene transfer. However, the characterization of the AAV preparations and the comparison of data between studies will become more complex without the appropriate use of common standards. As an example, here we have compared the vector genome titers and the capsid content of rAAV2RSM and rAAV8RSM using non-serotype-dependent techniques. This comparative study was performed in four institutions independently within the AAV8 RSM Working Group. The vector genome titer was measured by qPCR according to the SOPs written for the rAAV8RSM and using the primers and probe targeting the SV40 polyA. Of note, these experiments were performed before the collection of the data from the 16 laboratories and the statistical analysis shown in Table 4.

The vector genome titers of the rAAV8RSM obtained by the four laboratories were within the 95% confidence limits shown in Table 4; however, while the titers for the rAAV2RSM were within the confident limits in two laboratories, in two other institutions they were slightly lower than the lower confidence limit for the rAAV2RSM (2.7×10^{10} to 4.75×10^{10} vg/ml). Interestingly, the use of the rAAV2RSM as a control evidenced a significant deviation of the titration in the first assay conducted in Institution C (Table 5, in bold), and therefore the experiment was repeated. Altogether, these data indicate that the same protocol for vector titration by qPCR could be used independently of the serotype; however, the inclusion of one or more RSMs was crucial to obtain confident titers and avoid significant deviations.

Although the vector genome titer is the most widely used for dosing rAAV in clinical trials, it is also believed that total capsid content plays a critical role in the immune responses against the therapeutic vector (Manno *et al.*, 2006; Mingozzi *et al.*, 2007, 2009, 2013). Capsid titer can be measured by serotype-specific ELISA, as shown for rAAV2 (Grimm *et al.*, 1999; Lock *et al.*, 2010) and here for rAAV8; however, this assay is only available for several other serotypes, for example, AAV9, AAV1/6, AAV4, and AAV5 (Kuck *et al.*, 2007; Sonntag *et al.*, 2011), and it could be difficult to develop specific antibodies for hybrid/chimeric serotypes. Here, we have used SDS-PAGE gel and Sypro staining to semi-quantitate the capsid content of two different serotypes of AAV, in this case the rAAV2RSM and the rAAV8RSM. The same four institutions mentioned above performed this experiment. The same AAV8 vector stock used for the standard curve of the ELISA kit (WL217S) was used here as a control, with the exception that here the vector was used in its native form while the ELISA standard is supplied lyophilized. Notably, this experiment was performed before the collection of the data from the 16 laboratories and the statistical analysis shown in Table 4; thus, the rAAV2RSM sample was loaded on the gel according to the previously published capsid titer of 9.1×10^{11} pt/ml (Lock *et al.*, 2010), but the rAAV8RSM was loaded based on the capsid titer obtained in each institution using the specific AAV8 ELISA kit.

The amount of capsid of the rAAV2RSM was in agreement with the dose of WL217S used as standard, and, importantly, the amount of capsids loaded on the gel of the rAAV8RSM was similar to the rAAV2RSM (Fig. 3, and data not shown). Of

TABLE 5. TITRATION BY QPCR AAV2RSM VERSUS AAV8RSM

Laboratory	*Replicate*	*Genome titer AAV2RSM (qPCR) (vg/ml)*	*Genome titer AAV8RSM (qPCR) (vg/ml)*
A	1	2.37×10^{10}	7.91×10^{11}
	2	1.37×10^{10}	4.86×10^{11}
	3	2.83×10^{10}	5.39×10^{11}
	Mean	2.19×10^{10}	6.05×10^{11}
B	1	3.14×10^{10}	5.28×10^{11}
	2	2.03×10^{10}	2.26×10^{11}
	Mean	2.58×10^{10}	3.77×10^{11}
C	1	$\mathbf{1.56\times10^{11}}$	$\mathbf{4.55\times10^{12}}$
	2	$\mathbf{2.60\times10^{11}}$	$\mathbf{6.20\times10^{12}}$
C′	1′	3.18×10^{10}	5.76×10^{11}
	2′	3.11×10^{10}	5.58×10^{11}
	3′	3.40×10^{10}	5.60×10^{11}
	Mean	3.23×10^{10}	5.64×10^{11}
D	1	2.00×10^{10}	4.10×10^{11}
	2	3.80×10^{10}	4.20×10^{11}
	3	4.00×10^{10}	9.10×10^{11}
	mean	3.26×10^{10}	5.80×10^{11}

qPCR, quantitative polymerase chain reaction; RSM, Reference Standard Materials.

According to Lock *et al.* (2010), AAV2RSM qPCR titer with 95% confidence limits is 2.70×10^{10} vg/ml to 4.75×10^{10} vg/ml.

According to Table 4 in this article, AAV8RSM qPCR titer with 95% confidence is 3.05×10^{11} vg/ml to 1.09×10^{12} vg/ml.

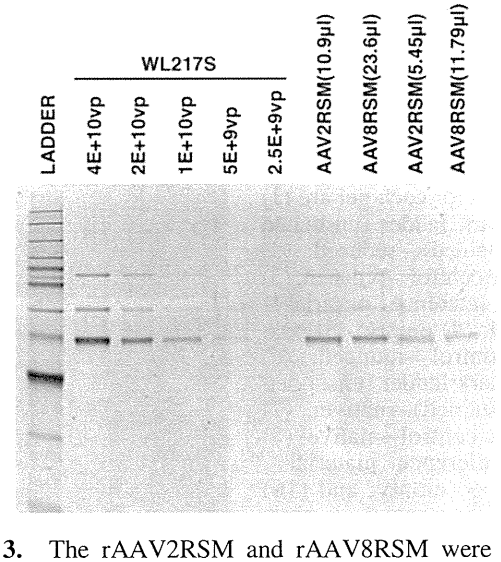

FIG. 3. The rAAV2RSM and rAAV8RSM were run on SDS-PAGE gels under denaturating conditions and then stained with Sypro Ruby. Several decreasing amounts of vector particles (pt) of a reference rAAV8 vector (WL217S) were loaded as standard curve (lanes 2–6). Different amounts (10^{10} pt or 5×10^{9} pt, lanes 7 and 8 or 9 and 10, respectively) of rAAV2RSM (lane 7 and 9) and rAAV8RSM (lane 8 and 10) were loaded on a gel according to a particle titer of 9.1×10^{11} pt/ml for rAAV2RSM (mean titer published by Lock *et al.*, 2010) and 4.2×10^{11} pt/ml for the rAAV8RSM (titer calculated by this lab using the ELISA AAV8).

note, the amount of vector genomes loaded on the SDS-PAGE gel was much higher for the rAAV8RSM than for the rAAV2RSM, since the rAAV2RSM had a much higher amount of empty capsids (Lock *et al.*, 2010). These data indicate that both ELISAs (AAV2 and the AAV8) generate comparable titers in terms of capsids/ml. These data also indicate that SDS-PAGE, a non-serotype-dependent technique, is useful to estimate the capsid content of rAAV vectors when specific antibodies (and therefore an ELISA) are not available.

Discussion

More than 100 clinical trials using different serotypes of rAAV have been registered up to 2014. Recently, a gene therapy product based on rAAV (Glybera) has been granted with the marketing authorization from the European Medicine Agency opening new dynamics and business models for rAAV-based therapeutics (Bryant *et al.*, 2013). Despite the extensive use of rAAV vectors, there has been a lack of standardization and inability to compare titer values for vectors made and tested within the same laboratory and within different ones. For this reason, an AAV2 Reference Standard Working group was formed in 2002 with the mission to generate and characterize an rAAV2RSM (Snyder *et al.*, 2002; Moullier *et al.*, 2008; Potter *et al.*, 2008). Sixteen laboratories participated in the characterization, and the consensus titers (and other characterization data) of rAAV2RSM were compiled and published (Lock *et al.*, 2010). However, vector systems based on novel rAAV serotypes (Gao *et al.*, 2002, 2004) are being developed rapidly and the scientific community raised the question of whether other RSM will be needed.

An AAV8RSM Working Group including industry and academic institutions from 10 countries and 16 laboratories was established in 2008 to generate and characterize an AAV8RSM (Moullier *et al.*, 2008, 2012; Ayuso *et al.*, 2012). Most of the members had participated in the AAV2RSM Working Group, which facilitated the effort and maintained continuity. Here, we have described the manufacturing and the characterization of a novel reference for the field, namely, the rAAV8RSM. The upstream process for the rAAV8RSM was based on cotransfection of HEK293 cells, as for the rAAV2RSM; but the downstream process was based on density gradient ultracentrifugation, which differs from the rAAV2RSM that was purified by chromatography (Potter *et al.*, 2008). Using the gradient purification protocol, we obtained an rAAV8RSM that is virtually free of empty capsids, which is a major difference compared with rAAV2RSM that contains more than 95% empty particles (Lock *et al.*, 2010). Another significant difference between the two standards is the ratio of vector genomes/infectious particles; this ratio is 7.5 for the rAAV2RSM but >400 for rAAV8RSM. We hypothesize that this is because of the poor ability for rAAV8 to transduce cells *in vitro*, as already described (Gao *et al.*, 2002; Mohiuddin *et al.*, 2005). Identifying cell lines that can be efficiently infected with different AAV serotypes and helper viruses is greatly needed, as this impacts not only the infectious titer values but also the particle to infectious ratio and transgene expression assays. However, as long as similar vector genome/infectious particle ratios are obtained for different lots of the same serotype, thus demonstrating lot-to-lot product consistency, and the ratios can be correlated to vector potency, then the vector lots can be considered suitable for use.

The characterization of the rAAV2RSM demonstrated a high degree of variation between institutions for each assay despite the relatively tight correlation of assay results within an institution. Here, we have observed exactly the same outcome during the characterization of the rAAV8RSM. This poor degree of interlaboratory precision and accuracy is very illuminating, in light of the major effort to standardize the assays by providing detailed protocols and common reagents. In addition, several laboratories had already performed the same assays in the frame of the rAAV2RSM project and the AAV2RSM was made available to the community before launching the characterization campaign of the rAAV8RSM.

Vector genome titer is the most commonly used titer to dose patients in clinical trials. Here, we observed a very significant variation of the vector genome titer by qPCR of the rAAV8RSM, with the lowest titer being 4.6×10^{10} vg/ml and the highest titer 4.7×10^{12} vg/ml (Table 3). Having a two-log difference in the titer of the same rAAV material is a cause for concern considering that most of the clinical trials use doses within one-log variation (Manno *et al.*, 2006; Nathwani *et al.*, 2011), and may reflect not only the qPCR variability itself (different PCR machines, different sources of PCR primers and probes, storage and handling of PCR reagents, preparation, and spectrophotometry of plasmid standard curves), but also rAAV sample preparation and recovery. qPCR has become the method of choice for AAV genome titration because of its simplicity and relative robustness. However, as we note here, the assay is not without sources of variability. As the field progresses, new and improved assays with greater degrees of precision are likely to emerge. In this regard, an AAV vector genome quantitation method based upon droplet digital PCR has recently been described, which yields improved intra- and interassay precision in comparison with qPCR, as well as eliminating the need for a plasmid standard curve (Lock *et al.*, 2014). Adoption of such techniques by the AAV gene therapy community may help to reduce the type of interlaboratory variation observed in this study.

The data presented here stress, more than ever, the necessity to work toward the calibration of vector titers and to standardize dosage units within the field. Now, two different rAAVRSMs are available to help validate in-house quantitative assays at a time where the field is maturing rapidly. As an example, four independent laboratories within the AAV8RSM working group performed an experiment consisting of titrating simultaneously the rAAV2RSM and the rAAV8RSM using the same protocols and reagents. The utilization of rAAV2RSM as a control permitted one laboratory to discard one of the tests that produced significant biased results with the overall result that the final titer of the rAAV8RSM obtained fell within the confidence limits for all 16 laboratories.

Interestingly, the capsid titer for both rAAV2RSM and rAAV8RSM determined by a commercial ELISA was the parameter with the least variation, perhaps because the kit provided the reagents and internal controls. Also, the capsid titers determined by the ELISA for serotype 2 and for the serotype 8 are comparable as showed by a non-serotype-dependent

methodology (Table 5). Quantification of total capsid content is critical for clinical trials, since immune responses are clearly dependent on the vector capsid (Manno *et al.*, 2006; Nathwani *et al.*, 2011). The availability of ELISA methods and RSMs will help the field to better characterize vector preparations used in clinical trials. Even if an ELISA is not available for a specific serotype or chimeric AAV vector, it is possible to use other methods to measure total capsids, such as electronic microscopy (see Materials and Methods section: rAAVSRSM characterization assays) (Grimm *et al.*, 1999), optical density (Sommer *et al.*, 2003), or SDS-PAGE gel staining (Fig. 3). rAAV2RSM and rAAV8RSM could be used to evaluate total capsid load for those alternative AAV serotypes.

A stability monitoring program that tracks physical and infectious titers over time is ongoing for the AAV2RSM generated in 2006, and data from several years have been collected (data not shown). Similarly, the AAV8RSM Working Group will follow the stability of the AAV8RSM at regular intervals.

Regulatory European (European Directorate for the Quality of Medicines [EDQM]) and U.S. (Food and Drug Administration [FDA], Center for Biologies Evaluation and Research [CBER], Office of Cellular, Tissue and Gene Therapies [OCTGT], and Division of Cellular and Gene Therapies [DCGT]) bodies have encouraged the AAV2RSM and AAV8RSM Working Group to generate and characterize reference materials and recommended the use of these standards to the sponsors of rAAV vector INDs and IMPDs.

In summary, this article describes the manufacturing and the characterization of a novel rAAV8RSM material deposited at ATCC under the reference VR-1816 that represents an important tool to better determine vector dosing units. Having validated and calibrated methods to determine rAAV titers of preclinical and clinical vectors will accelerate the development of rAAV-based medicines and will protect patients participating in future trials.

Acknowledgments

This work was supported by the Clinigene network of excellence (European Commission FP6, Clinigene, LSHB-CT-2006-018933). We thank Odile Cohen-Haguenauer for conceiving, writing, and submitting the Clinigene European Network of Excellence. We also thank the support of several partners of the Clinigene AAV platform to the AAV8RSM project: Robin Ali, Muriel Audit, George Dickson, Anne Douar, Amit Nathwani, Amos Panet, Thierry Vandendriessche, and Bas Blits.

We are also indebted to Liz Kerrigan at ATCC for coordinating the distribution of materials to testing laboratories, and Keith Carson (ISBiotech) and Denise Gavin (FDA) for useful discussions and guidance. We acknowledge the generosity of members of the AAV RSM Working Group who participated in the production and characterization of the rAAV8RSM.

We acknowledge the technical help of the following during the manufacturing and testing phase: Maria Molas, Jose Piedra, Katell Konan, Armelle Cassard, Solene Volant, Linda Poiraudeau, Frederic Broucque, Emilie Lecomte, Achille François, Antonella Ferrara, Diana Desgue, Marina Dapas, Michela Zotti, Rachida Siamari, Saskia Haast, Wienman Philips, and Albertine de Jong.

We acknowledge the generosity of PROGEN, ATCC, PlasmidFactory, Corning, PAA, SGS-Vitrology, Labclinics, and Clean Cells for providing free access to materials and reagents required for the production and characterization of the AAV8RSM.

Author Disclosure Statement

Richard Snyder owns equity in a gene therapy company that is commercializing AAV for gene therapy applications. J. Fraser Wright is scientific cofounder of and consultant to Spark Therapeutics, a gene therapy company. All other authors declare no conflict of interest.

References

ATCC Virus Reference Materials. Available at: www.lgcstandards-atcc.org/Standards/Standards_Programs/ATCC_Virus_Reference_Materials (accessed Oct. 24, 2014).

Ayuso, E., Mingozzi, F., Montane, J., *et al.* (2010). High AAV vector purity results in serotype- and tissue-independent enhancement of transduction efficiency. Gene Ther. 17, 503–510.

Ayuso, E., Blouin, V., Darmon, C., *et al.* (2012). Reference materials for the characterization of adeno-associated viral vectors. In *The Clinibook: Clinical Gene Transfer State of the Art.* O. Cohen-haguenauer, ed. (EDK, Paris) *pp.* 83–90.

Bainbridge, J.W., Smith, A.J., Barker, S.S., *et al.* (2008). Effect of gene therapy on visual function in Leber's congenital amaurosis. N. Engl. J. Med. 358, 2231–2239.

Bryant, L.M., Christopher, D.M., Giles, A.R., *et al.* (2013). Lessons learned from the clinical development and market authorization of Glybera. Hum. Gene Ther. Clin. Dev. 24, 55–64.

Burger, C., Gorbatyuk, O.S., Velardo, M.J., *et al.* (2004). Recombinant AAV viral vectors pseudotyped with viral capsids from serotypes 1, 2, and 5 display differential efficiency and cell tropism after delivery to different regions of the central nervous system. Mol. Ther. 10, 302–317.

Gao, G.P., Alvira, M.R., Wang, L., *et al.* (2002). Novel adeno-associated viruses from rhesus monkeys as vectors for human gene therapy. Proc. Natl. Acad. Sci. USA 99, 11854–11859.

Gao, G., Vandenberghe, L.H., Alvira, M.R., *et al.* (2004). Clades of Adeno-associated viruses are widely disseminated in human tissues. J. Virol. 78, 6381–6388.

Gaudet, D., Methot, J., Dery, S., *et al.* (2013). Efficacy and long-term safety of alipogene tiparvovec (AAV1-LPLS447X) gene therapy for lipoprotein lipase deficiency: an open-label trial. Gene Ther. 20, 361–369.

Grimm, D., Kern, A., Pawlita, M., *et al.* (1999). Titration of AAV-2 particles via a novel capsid ELISA: packaging of genomes can limit production of recombinant AAV-2. Gene Ther. 6, 1322–1330.

Hutchins, B. (2002). Development of a reference material for characterizing adenovirus vectors. BioProcess J. 1, 25–29.

Kuck, D., Kern, A., and Kleinschmidt, J.A. (2007). Development of AAV serotype-specific ELISAs using novel monoclonal antibodies. J. Virol. Methods 140, 17–24.

Littell, R.C., Milliken, G.A., Stroup, W.W., *et al.* (2006). *SAS for Mixed Models*, 2nd edition. (SAS Institute, Inc., Cary, NC).

Lock, M., McGorray, S., Auricchio, A., *et al.* (2010). Characterization of a recombinant adeno-associated virus type 2 Reference Standard Material. Hum. Gene Ther. 21, 1273–1285.

Lock, M., Alvira, M.R., Chen, S.J., *et al.* (2014). Absolute determination of single-stranded and self-complementary adeno-associated viral vector genome titers by droplet digital PCR. Hum. Gene Ther. Methods 25, 115–125.

Maguire, A.M., Simonelli, F., Pierce, E.A., *et al.* (2008). Safety and efficacy of gene transfer for Leber's congenital amaurosis. N. Engl. J. Med. 358, 2240–2248.

Manno, C.S., Arruda, V.R., Pierce, G.F., *et al.* (2006). Successful transduction of liver in hemophilia by AAV-Factor IX and limitations imposed by the host immune response. Nat. Med. 12, 342–347.

Mingozzi, F., Maus, M.V., Hui, D.J., *et al.* (2007). CD8(+) T-cell responses to adeno-associated virus capsid in humans. Nat. Med. 13, 419–422.

Mingozzi, F., Meulenberg, J.J., Hui, D.J., *et al.* (2009). AAV-1-mediated gene transfer to skeletal muscle in humans results in dose-dependent activation of capsid-specific T cells. Blood 114, 2077–2086.

Mingozzi, F., Anguela, X.M., Pavani, G., *et al.* (2013). Overcoming preexisting humoral immunity to AAV using capsid decoys. Sci. Transl. Med. 5, 194ra92.

Mohiuddin, I., Loiler, S., Zolotukhin, I., *et al.* (2005). Herpesvirus-based infectious titering of recombinant adeno-associated viral vectors. Mol. Ther. 11, 320–326.

Moullier, P., and Snyder, R.O. (2008). International efforts for recombinant adeno-associated viral vector reference standards. Mol. Ther. 16, 1185–1188.

Moullier, P., and Snyder, R.O. (2012). Recombinant adeno-associated viral vector reference standards. Methods Enzymol. 507, 297–311.

Nathwani, A.C., Tuddenham, E.G., Rangarajan, S., *et al.* (2011). Adenovirus-associated virus vector-mediated gene transfer in hemophilia B. N. Engl. J. Med. 365, 2357–2365.

Potter, M., Phillipsber, G., Phillipsberg, T., *et al.* (2008). Manufacture and stability study of the recombinant adeno-associated virus serotype 2 reference standard. Bioprocessing J. 7, 8–14.

Rabilloud, T., Strub, J.M., Luche, S., *et al.* (2001). A comparison between Sypro Ruby and ruthenium II tris (bathophenanthroline disulfonate) as fluorescent stains for protein detection in gels. Proteomics 1, 699–704.

Snyder, R.O., and Flotte, T.R. (2002). Production of clinical-grade recombinant adeno-associated virus vectors. Curr. Opin. Biotechnol. 13, 418–423.

Sommer, J.M., Smith, P.H., Parthasarathy, S., *et al.* (2003). Quantification of adeno-associated virus particles and empty capsids by optical density measurement. Mol. Ther. 7, 122–128.

Sonntag, F., Kother, K., Schmidt, K., *et al.* (2011). The assembly-activating protein promotes capsid assembly of different adeno-associated virus serotypes. J. Virol. 85, 12686–12697.

Tessier, J., Chadeuf, G., Nony, P., *et al.* (2001). Characterization of adenovirus-induced inverted terminal repeat-independent amplification of integrated adeno-associated virus rep-cap sequences. J. Virol. 75, 375–383.

Vandenberghe, L.H., Xiao, R., Lock, M., *et al.* (2010). Efficient serotype-dependent release of functional vector into the culture medium during adeno-associated virus manufacturing. Hum. Gene Ther. 21, 1251–1257.

Van Vliet, K., Blouin, V., Agbandje-McKenna, M., *et al.* (2006). Proteolytic mapping of the adeno-associated virus capsid. Mol. Ther. 14, 809–821.

Weiss, W., Weiland, F., and Gorg, A. (2009). Protein detection and quantitation technologies for gel-based proteome analysis. Methods Mol. Biol. 564, 59–82.

Address correspondence to:
Dr. Philippe Moullier
INSERM UMR 1089
Institut de Recherche Thérapeutique
Université de Nantes
8, quai Moncousu–6ème Etage
BP 70721
44007 NANTES Cedex 1
France

E-mail: moullier@ufl.edu

Dr. Richard Snyder
Department of Molecular Genetics and Microbiology
University of Florida College of Medicine
1600 SW Archer Road
Gainesville, FL 32610-0266

E-mail: rsnyder@cerhb.ufl.edu

Received for publication May 29, 2014;
accepted after revision September 23, 2014.

Published online: September 30, 2014.

Gene Therapy (2015) **22,** 209–215

www.nature.com/gt

SHORT COMMUNICATION

The *Tol2* transposon system mediates the genetic engineering of T-cells with CD19-specific chimeric antigen receptors for B-cell malignancies

T Tsukahara[1,2], N Iwase[1], K Kawakami[3], M Iwasaki[3], C Yamamoto[1,4], K Ohmine[2,4], R Uchibori[1,2], T Teruya[2], H Ido[2], Y Saga[1,5], M Urabe[1], H Mizukami[1], A Kume[1], M Nakamura[6], R Brentjens[7] and K Ozawa[1,2,4]

Engineered T-cell therapy using a CD19-specific chimeric antigen receptor (CD19-CAR) is a promising strategy for the treatment of advanced B-cell malignancies. Gene transfer of CARs to T-cells has widely relied on retroviral vectors, but transposon-based gene transfer has recently emerged as a suitable nonviral method to mediate stable transgene expression. The advantages of transposon vectors compared with viral vectors include their simplicity and cost-effectiveness. We used the *Tol2* transposon system to stably transfer CD19-CAR into human T-cells. Normal human peripheral blood lymphocytes were co-nucleofected with the *Tol2* transposon donor plasmid carrying CD19-CAR and the transposase expression plasmid and were selectively propagated on NIH3T3 cells expressing human CD19. Expanded $CD3^+$ T-cells with stable and high-level transgene expression (~95%) produced interferon-γ upon stimulation with CD19 and specifically lysed Raji cells, a $CD19^+$ human B-cell lymphoma cell line. Adoptive transfer of these T-cells suppressed tumor progression in Raji tumor-bearing $Rag2^{-/-}\gamma c^{-/-}$ immunodeficient mice compared with control mice. These results demonstrate that the *Tol2* transposon system could be used to express CD19-CAR in genetically engineered T-cells for the treatment of refractory B-cell malignancies.

Gene Therapy (2015) **22,** 209–215; doi:10.1038/gt.2014.104; published online 27 November 2014

INTRODUCTION

Adoptive immunogene therapy with T-cells expressing chimeric antigen receptors (CARs) is a promising approach for the treatment of advanced malignancies. CARs are composed of an extracellular single chain fragment of variable region fused to one of the two intracellular lymphocyte signaling domains, CD28 or 4-1BB (CD137), coupled with CD3ζ to mediate T-cell activation.[1] T-cells transduced with CAR-expressing vectors can recognize and kill tumor cells that express tumor-associated antigens such as CD19 in a human leukocyte antigen-independent manner. In early-phase clinical trials, the adoptive transfer of CD19-specific CAR (CD19-CAR)-transduced T-cells was found to cause anti-tumor effects in patients with chemorefractory $CD19^+$ B-cell malignancies.[2]

The gene transfer of CARs into T-cells has mainly been achieved using retroviral vectors. However, DNA transposon-based gene transfer has emerged as an appealing alternative, because transposon vectors are easier and less expensive to manufacture than retroviral vectors.[3] Transposon vectors work via a cut-and-paste mechanism called transposition, whereby transposon DNA containing the gene of interest is integrated into chromosomal DNA by a transposase.

Tol2 is an active transposon derived from the medaka fish (*Oryzias latipes*).[3,4] It is active in a variety of vertebrate species and has been used for gene transfer in mammalian cells.[4,5] *Tol2* has a fairly large cargo capacity; it can carry a total of around 200 kb and ~10 kb without reducing its transpositional activity.[6,7] Recently, the piggyBac (PB) transposon was shown to have a cargo capacity of 150 kb.[8] Transposase itself can act as a transposition inhibitor when it exceeds a threshold concentration, enabling it to limit transposon activity in a phenomenon called overproduction inhibition (OPI). The Sleeping Beauty (SB) transposon undergoes OPI, whereas *Tol2* and PB transposons exhibit limited OPI.[9] Unlike SB and PB transposons that specifically integrate at TA or TTAA sequences, respectively, *Tol2* does not appear to have a specific preferential target sequence.[3]

In the present study, we investigated whether the *Tol2* transposon system could mediate the stable transfer of CD19-CAR to primary human T-cells. We show that *Tol2*-engineered T-cells efficiently and stably expressed CD19-CAR and exhibited CD19-dependent anti-tumor effects *in vitro* and in a mouse xenograft model. Our results demonstrate for the first time that the *Tol2* transposon system can be used to stably express CD19-CAR in engineered T-cells for the treatment of B-cell malignancies.

RESULTS AND DISCUSSION

Transposons are promising nonviral vectors for human gene therapy. They have significantly higher integration efficiencies than electro-transferred naked DNA plasmids. Moreover, compared with retroviral vectors, transposons offer several

[1]Division of Genetic Therapeutics, Center for Molecular Medicine, Jichi Medical University, Shimotsuke, Tochigi, Japan; [2]Division of Immuno-Gene and Cell Therapy (Takara Bio), Jichi Medical University, Shimotsuke, Tochigi, Japan; [3]Division of Molecular and Developmental Biology, National Institute of Genetics, Mishima, Shizuoka, Japan; [4]Division of Hematology, Department of Medicine, Jichi Medical University, Shimotsuke, Tochigi, Japan; [5]Department of Obstetrics and Gynecology, Jichi Medical University, Shimotsuke, Tochigi, Japan; [6]Human Gene Sciences Center, Tokyo Medical and Dental University, Bunkyo-ku, Tokyo, Japan and [7]Department of Medicine, Memorial Sloan Kettering Cancer Center, New York, NY, USA. Correspondence: Dr T Tsukahara, Division of Genetic Therapeutics, Center for Molecular Medicine, Jichi Medical University, 3311-1 Yakushiji, Shimotsuke, Tochigi 329-0498, Japan.
E-mail: ttsukahara@ jichi.ac.jp
Received 31 March 2014; revised 29 September 2014; accepted 21 October 2014; published online 27 November 2014

advantages, such as low immunogenicity, simplicity of use and low manufacturing costs. The SB and PB transposon systems have also been used to stably introduce CD19-CARs into human T-cells,[10,11] while the SB system recently formed part of a human clinical trial involving CAR-based T-cell therapy for B-cell malignancies.[12]

In the present study, we generated a *Tol2* transposon construct carrying the *CD19-CAR* gene (pTol2-CD19-CAR) (Figure 1). To evaluate whether the *Tol2* transposon system could be used for *CD19-CAR* transfer, human peripheral blood lymphocytes (PBLs) were transfected with pTol2-CD19-CAR in the presence or absence of the *Tol2* transposase expression plasmid (pCAGGS-mT2TP) (Figure 1). Transfected T-cells were propagated on NIH3T3 cells expressing CD19 (3T3/CD19).

We analyzed the surface expression of CD19-CAR in transfected T-cells by flow cytometry. On day 21 of the culture, CD19-CAR$^+$ CD3$^+$ T-cells constituted approximately 95% of cultures transfected with both *Tol2* transposon and transposase plasmids, whereas CD19-CAR expression was very low (2%) in T-cells transfected with the transposon alone (Figure 2a). We also confirmed CD19-CAR expression in T-cells co-transfected with *Tol2* transposase by western blotting (Figure 2b). Co-transfected T-cells showed an approximately 29-fold expansion within 3 weeks, while T-cells transfected with transposon alone did not grow (Figure 2c). We next examined the immunophenotypes of expanded T-cells by flow cytometry. On day 21, these T-cells were positive for CD3 (99%), CD4 (61%) and CD8 (34%) after *ex vivo* expansion with antigen stimulation (Supplementary Figure S1). A CD4-dominant population was also previously observed in the results of SB- and PB-based T-cell gene transfer with CD19-CAR,[10,13] while Saito *et al.*[14] recently showed a CD8-dominant culture method after PB-based T-cell gene transfer with CD19-CAR. When specific T-cell subsets of engineered T-cells were analyzed in the present study, both CD45RO$^+$CD62L$^+$ central memory and CD45RO$^+$CD62L$^-$ effector memory phenotypes were present (Supplementary Figure S1). These results show that large numbers of T-cells with stable and high-level transgene expression were generated by *Tol2*-mediated gene transfer and *ex vivo* expansion.

To examine whether stable CD19-CAR expression in *Tol2*-engineered T-cells was caused by genomic integration of the transposon, we measured the transgene copy number relative to the copy number of the interferon (*IFN*)-*γ* gene as a reference using real-time quantitative PCR. At 21 and 29 days posttransduction, the calculated transgene copies per T-cell were 1.75 ± 0.1 and 1.53 ± 0.6 (mean ± s.d., $n = 3$), respectively, for the *Tol2*-mediated gene transfer samples. We also mapped the transposon integration sites in these T-cells (day 29) by inverse PCR, as well as the integration sites of CD19-CAR T-cells generated by the retrovirus system in our previous study[15] as a control (Table 1). These results indicate that the *Tol2* transposon integrated into the human genome and stably expressed CD19-CAR in primary human T-cells.

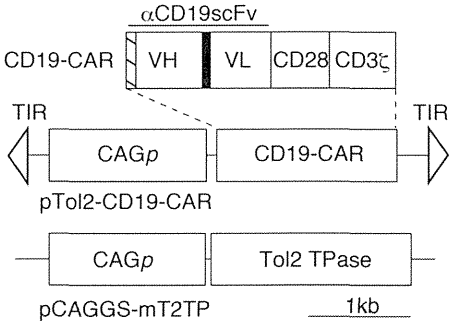

Figure 1. CD19-CAR and the *Tol2* transposon system used in this study. VH, variable heavy chain; VL, variable light chain; hatched box, CD8α signal peptide; black box, $(GGGGS)_3$ linker; pTol2-CD19-CAR, *Tol2* transposon plasmid carrying *CD19-CAR*; CAG*p*, hybrid cytomegalovirus enhancer/chicken β-actin promoter; TIR, terminal inverted repeat; pCAGGS-mT2TP, *Tol2* transposase (TPase) expression plasmid.

We next assessed antigen-dependent IFN-γ production of *Tol2*-engineered T-cells by enzyme-linked immunosorbent assay and found that they selectively produced IFN-γ only in response to CD19$^+$ target cells (Figure 3a). CD19-CAR T-cells showed cell lytic activity against Raji cells but not against control CD19-negative K562 cells (Figure 3b). We then examined which subpopulations of T-cells were involved in targeted cell killing by cell fractionation. Both CD4$^+$- and CD8$^+$-sorted T-cells specifically lysed CD19$^+$ target cells. However, CD4$^+$ T-cell-mediated cytotoxicity was about twofold less than that observed for CD8$^+$ T-cells (Figure 3c). Moreover, CD4$^+$ and CD8$^+$ T-cells also killed primary CD19$^+$ B-cell lymphoma cells isolated from a patient with a diffuse large B-cell lymphoma (Figure 3d). Taken together, these results demonstrate that expanded CD19-CAR T-cells exhibited CD19-dependent effector functions *in vitro*.

We next wanted to evaluate the *in vivo* anti-tumor effects of engineered T-cells in a mouse xenograft model that we previously established.[15] Rag2$^{-/-}$γc$^{-/-}$ immunodeficient mice were intravenously injected with luciferase-expressing Raji cells. Three days later, the mice were intravenously injected with CD19-CAR T-cells. Bioluminescent imaging revealed that CD19-CAR T-cells successfully suppressed Raji tumor progression, while Raji tumors grew systemically in the untreated group (Figure 4a). To augment these *in vivo* findings, we evaluated treatment with an antibody against the programmed death (PD)-1 protein, because our expanded T-cells partially expressed PD-1 (23 ± 6.2%; mean ± s.d., $n = 3$) and a PD-1 blockade by the antibody previously enhanced the anti-tumor activity of PD-1$^+$ tumor- or virus-specific T-cells *in vivo*.[16] We found that use of the anti-PD-1 antibody did not significantly reduce the number of tumors at the day 27 end point compared with the T-cell group alone ($P = 0.30$) (Figures 4a and b). However, two of the four animals treated with the anti-PD-1 antibody were tumor free, while all three mice in the T-cell group carried tumors. These observations do not support those of John *et al.*,[17] who previously demonstrated that treatment with an anti-PD-1 antibody augmented the anti-tumor activity of PD-1$^+$ Her-2-specific CAR T-cells cultured with antigen stimulation in their mouse model of Her-2$^+$ breast cancer. It is possible that the types of tumors, levels of PD-1 and use of immunocompetent or immunocompromised animals in these different studies may account for these observed differences. Neither nontransduced T-cells nor the PD-1 antibody injection alone suppressed tumor progression in our present study (data not shown).

We next examined whether interleukin (IL)-7 could improve the *in vivo* efficacy of these T-cells in our mouse model, because IL-7 has been used to augment the anti-tumor effects of antigen-specific T-cells after adoptive cell therapy in mouse models.[18] We used the adeno-associated virus (AAV) vector system to achieve systemic and long-term IL-7 expression in mice.[19] The IL-7+ T-cell group showed enhanced tumor suppression via imaging analysis compared with that of the control group ($P = 0.001$) and approached statistical significance compared with that of the T-cell transfer group alone ($P = 0.12$, Figures 4c and d). AAV-mediated IL-7 administration alone did not suppress tumor growth (data not shown). These results show that *Tol2*-engineered T-cells function as anti-tumor effector cells in our mouse model.

CAR-based T-cell therapy is dependent on efficient gene transfer and an optimal expansion regimen to achieve both the cell number and potency required for use in the clinical setting. One day after nucleofection, expression of CD19-CAR was ~24% in CD3$^+$ *Tol2*-engineered T-cells (Figure 2a, upper), which is similar to the transgene expression previously observed in

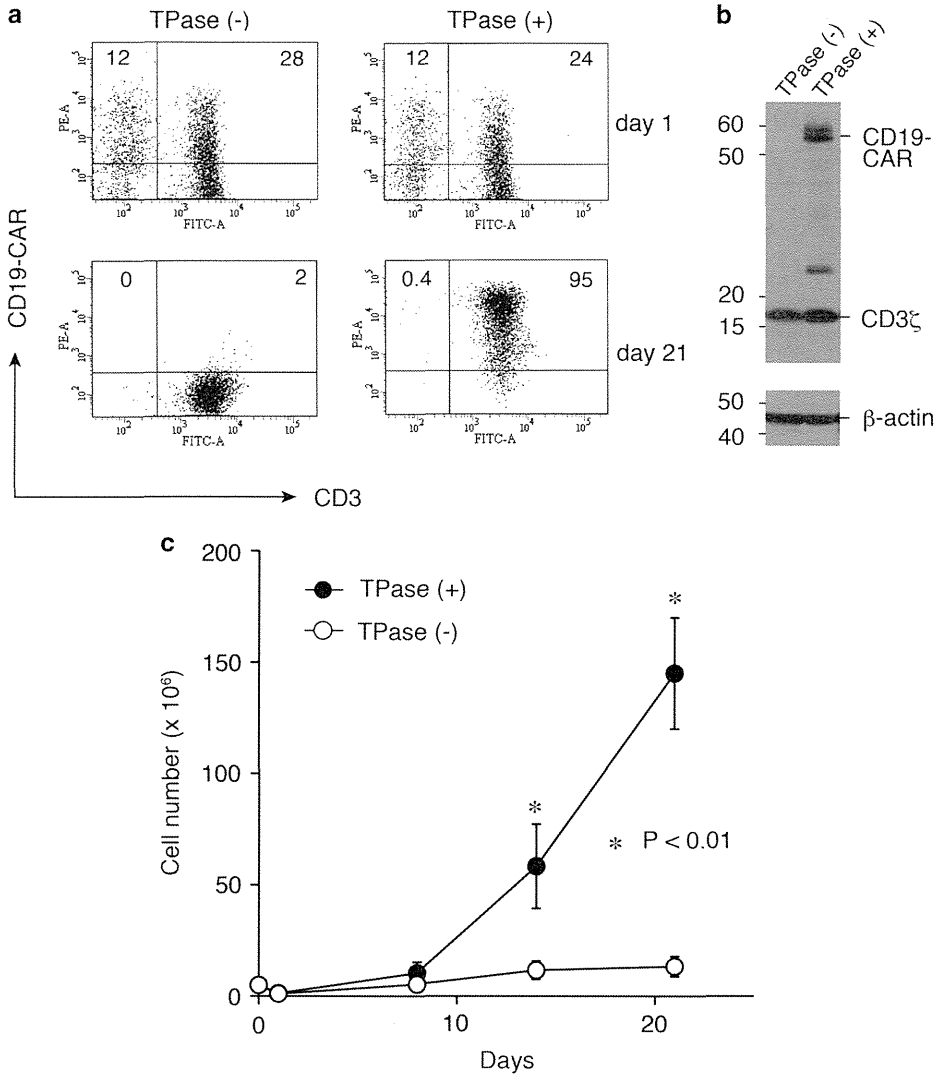

Figure 2. CD19-CAR expression and *ex vivo* expansion of *Tol2*-modified T-cells. (**a**) Surface expression of CD19-CAR on T-cells after nucleofection with pTol2-CD19-CAR with or without pCAGGS-mT2TP (TPase) plasmids was examined by flow cytometry. Values represent the percentages of $CD3^+$ $CD19\text{-}CAR^+$ and $CD3^-$ $CD19\text{-}CAR^+$ cells. Data are representative of one of the three independent experiments using different donors. (**b**) CD19-CAR expression of *Tol2*-tranduced T-cells in the presence or absence of TPase as detected by western blotting with an anti-CD3ζ antibody. β-Actin was used as a loading control. (**c**) Growth rates of transduced T-cells with or without TPase. 3T3/CD19 cells were added weekly. Viable cells were enumerated by trypan blue exclusion. Data represent mean ± s.d. from three different donors.

Table 1. Integration sites in *Tol2*- and retrovirus-modified T-cells

Vector	*Clone*	*RefSeq gene*	*RefSeq no.*	*Location*	*Chromosome*
Tol2	No. 1	FAM46A	NM_017633.2	Intron 1	6
	No. 2	MFI2	NM_005929.5	Intron 1	3
	No. 3	VGLL1	NM_016267.3	20.6 kb 3′	X
	No. 4	ZMPSTE24	NM_005857.4	0.6 kb 5′	1
	No. 5	CDH23	NM_001171930.1	Intron 25	10
	No. 6	TMEM200A	NM_001258276.1	Exon 1	6
Retrovirus	No. 7	FYB	NM_001243093.1	Intron 1	5
	No. 8	BRE	NM_001261840.1	Intron 10	2
	No. 9	ZNF706	NM_001042510.1	40.6 kb 3′	8
	No. 10	SLFN5	XM_005257934.1	12.8 kb 3′	17
	No. 11	NF1	NM_000267.3	Intron 36	17

Distance from the transcription start site or end sites of RefSeq genes is indicated.